Clinical Science (2017) **131** 2763–2775
https://doi.org/10.1042/CS20171252

PORTLAND PRESS

Research Article

Regulation of human feto-placental endothelial barrier integrity by vascular endothelial growth factors: competitive interplay between VEGF-A_{165}a, VEGF-A_{165}b, PlGF and VE-cadherin

Vincent Pang[1,2], David O. Bates[1] and Lopa Leach[2]

[1]Cancer Biology, Division of Cancer and Stem Cells, School of Medicine, University of Nottingham, Queen's Medical Centre, Nottingham NG2 7UH, U.K.; [2]School of Life Sciences, University of Nottingham, Queen's Medical Centre, Nottingham NG2 7UH, U.K.

Correspondence: David O. Bates (David.Bates@nottingham.ac.uk) or Lopa Leach (Lopa.Leach@nottingham.ac.uk)

The human placenta nourishes and protects the developing foetus whilst influencing maternal physiology for fetal advantage. It expresses several members of the vascular endothelial growth factor (VEGF) family including the pro-angiogenic/pro-permeability VEGF-A_{165}a isoform, the anti-angiogenic VEGF-A_{165}b, placental growth factor (PlGF) and their receptors, VEGFR1 and VEGFR2. Alterations in the ratio of these factors during gestation and in complicated pregnancies have been reported; however, the impact of this on feto-placental endothelial barrier integrity is unknown. The present study investigated the interplay of these factors on junctional occupancy of VE-cadherin and macromolecular leakage in human endothelial monolayers and the perfused placental microvascular bed. Whilst VEGF-A_{165}a (50 ng/ml) increased endothelial monolayer albumin permeability ($P<0.0001$), equimolar concentrations of VEGF-A_{165}b ($P>0.05$) or PlGF ($P>0.05$) did not. Moreover, VEGF-A_{165}b (100 ng/ml; $P<0.001$) but not PlGF (100 ng/ml; $P>0.05$) inhibited VEGF-A_{165}a-induced permeability when added singly. PlGF abolished the VEGF-A_{165}b-induced reduction in VEGF-A_{165}a-mediated permeability ($P>0.05$); PlGF was found to compete with VEGF-A_{165}b for binding to Flt-1 at equimolar affinity. Junctional occupancy of VE-cadherin matched alterations in permeability. In the perfused microvascular bed, VEGF-A_{165}b did not induce microvascular leakage but inhibited and reversed VEGF-A_{165}a-induced loss of junctional VE-cadherin and tracer leakage. These results indicate that the anti-angiogenic VEGF-A_{165}b isoform does not increase permeability in human placental microvessels or HUVEC primary cells and can interrupt VEGF-A_{165}a-induced permeability. Moreover, the interplay of these isoforms with PlGF (and s-flt1) suggests that the ratio of these three factors may be important in determining the placental and endothelial barrier in normal and complicated pregnancies.

Received: 28 July 2017
Revised: 03 October 2017
Accepted: 19 October 2017

Accepted Manuscript Online: 20 October 2017
Version of Record published: 23 November 2017

Introduction

The human placenta is a fetal organ which allows oxygen and selective nutrient uptake from the mother to the fetus, whilst acting as a discriminatory barrier. It does this by having a unique architecture, specific to human and macaque monkeys, where the placental microvessels, encased in a single layer of syncytiotrophoblast, lie bathed in maternal blood (haemomonochorial). fetal blood enters these vessels through the umbilical arteries and returns replenished via the umbilical vein. Both the thin outer syncytial lining and the fetal endothelium act as resistance in series to transport of hydrophilic solutes from

PORTLAND PRESS

Clinical Science (2017) **131** 2763–2775
https://doi.org/10.1042/CS20171252

maternal to fetal blood [1]. The feto-placental endothelial barrier integrity is therefore of critical importance to fetal growth and well-being.

The placental endothelium is continuous, with well-defined cell–cell junctions that restrict movement of large hydrophilic molecules (>65 kDa) across the paracellular cleft [2]. Adherens junctions (AJs) are the major regulators of paracellular permeability in the placental capillaries with the transmembrane adhesion molecule – vascular endothelial (VE)-cadherin being the key player [3-5]. Phosphorylation of VE-cadherin leads to breakage of homophilic binding, loss of anchorage to peri-junctional actin and translocation from AJ domains with accompanying increases in paracellular cleft dimensions and increased paracellular permeability [6]. VEGF-A, via stimulation of VEGFR2, has been shown to increase phosphorylation of VE-cadherin at Tyr-685 and Tyr-731 facilitating increased solute permeability and extravasation of cells [7].

The human placenta expresses the pro-angiogenic/pro-permeability VEGF-A_{165}a, anti-angiogenic VEGF-A_{165}b, placental growth factor (PIGF) and their receptors, VEGFR2 (KDR), VEGFR1 (Flt-1), neuropilin-1 and soluble Flt-1 (sFlt-1). There is differential expression of the growth factors during gestation and in complicated pregnancies. VEGF-A levels are highest in the first trimester during *de novo* synthesis of placental vessels [8,9]). The *in situ* location also alters with gestation; in the last trimester VEGF-A is found predominantly in the terminal villi which house dilated fetal capillary loops involved in materno-fetal exchange [10]. Elevated levels of VEGF-A, loss of junctional VE-cadherin and increased vascular leakage have been reported in pregnancies complicated by maternal diabetes ([11,12]) whilst trophoblast derived factors from pre-eclamptic placenta have been shown to diminish barrier function and alter VE-cadherin distribution *in vitro* [13]. The anti-angiogenic splice variant VEGF-A_{165}b has been shown to be present in human term placentae as a small part of the total VEGF expression. Interestingly, there is a further down-regulation of this in pre-eclamptic placenta [14]. Whether this splice-variant can affect placental vascular permeability is not known.

PIGF, a homologue of VEGF [15], rises steadily until the second trimester of pregnancy – a period of maximal vessel maturation and then begins to fall [16]. Lower PIGF levels in maternal circulation have been correlated with small-for-gestational-age babies in normal pregnancies [17,18]. A down-regulation of syncytiotrophoblast PlGF was found in pre-eclamptic placenta [19]. Its function in the placenta remains to be shown experimentally. Of the various isoforms of PIGF, PIGF-2 is thought to enhance VEGF-induced permeability, whilst PIGF promotes VEGF-induced angiogenesis in some models and antagonizes in others [20,15]).

The interplay of VEGF-A_{165}a, VEGF-A_{165}b and PIGF depend largely on their interactions with their receptors and co-receptors. VEGF-A_{165}a is able to bind to both VEGFR1 and R2 but acts mainly via the latter [21]. Interestingly, neuropilin-1 can complex with VEGFR1 and R2 and has been shown to potentiate VEGFR2 activation [22]. VEGF-A_{165}b binds to both VEGFR1 and R2 receptors but is a weaker agonist for VEGFR2 [23]. VEGF-A_{165}b differs from VEGF-A_{165}a only in the last six amino acids, the residues necessary for interaction with neuropilin-1, [24-26] and this lack of co-receptor binding may be behind its function as a partial receptor agonist. PlGF only binds to VEGFR1 but has been shown to propagate kinase cascades for VE-cadherin autophosphorylation [27]. The competitive interplay between the VEGF splice variants and PIGF in regulation of human placental endothelial junctional integrity requires elucidation.

The aim of the present study was therefore to investigate whether VEGF-A_{165}a, VEGF-A_{165}b and PlGF, singly or in combination can affect junctional occupancy of VE-cadherin and alter paracellular permeability of human placental/fetal endothelium. Term placenta and umbilical cord from healthy pregnancies were used for *ex vivo* placental perfusion experiments and for endothelial primary cell culture studies. Results obtained will advance understanding of the mechanisms employed by the human placenta for maintenance of the feto-placental endothelial barrier and how this could be perturbed in complicated pregnancies.

Methodology

Placenta and umbilical cord collection

Term placentas and umbilical cords were obtained at elective caesarean section from normal pregnancies with informed patient consent and full ethical approval (REC Ref 14/SC/ 1194; NHS Heath Research Authority, U.K.), and permission from Nottingham University Hospitals, NHS Trust, U.K. The work described here has been carried out in accordance with The Code of Ethics of the World Medical Association (Declaration of Helsinki).

All term placentas and umbilical cords were obtained from term (≥37 weeks), non-labouring women (Table 1) undergoing scheduled elective caesarean section delivery. Indications for caesarean section include maternal request, breech presentation, and previous caesarean section. Women with pre-existing conditions such as hypertension

Table 1 The characteristics of patients undergoing caesarean deliveries who participated in the present study, and whose data were used for further analysis

Age (years)	29.5 ± 4.7
BMI	25.6 ± 2.4
Parity	2 [2–3]
Gestational age (weeks)	40.6 ± 3.5
Weight of placenta (g)	701.33 ± 78.5
Sex of offspring:	
Male	37.5%
Female	62.5%
Weight of offspring (kg)	3.3 ± 0.6

BMI, body mass index; data reported as mean ± the standard deviation (SD), median [Interquartile range (IQR)], or percentage of offspring.

(>140/90 mmHg), proteinuria, diabetes, gestational diabetes, renal and cardiac disease, and other conditions that may compromise patient health were excluded. Smokers were excluded from the study.

Primary cell culture

Human umbilical vein endothelial cell (HUVECs) were isolated from freshly delivered umbilical cords and cultured on 1% gelatin-coated flasks in complete endothelial cell medium M199 (Gibco), supplemented with 20% fetal bovine serum (FBS), heparin sodium salt (50 μg/ml), endothelial cell growth factor supplement (50 μg/ml), and penicillin/streptomycin (100 U/100 mg/ml), under humidified conditions at 37°C and 5% CO_2/95% air. In all experiments, HUVECs were grown and used only up to the third passage.

HUVEC permeability assays

Polyester membrane transwell 6.5 mm^2 inserts with a 0.4 μm pore diameter (Corning, U.K.) were coated with 1% gelatin in 0.1 M PBS. They were suspended in a 24-well cell culture plates and seeded with 5×10^3 cells. Hundred microlitres of complete endothelial cell medium M199 was added to the upper compartment and 400 μl added to lower compartment to equalize hydrostatic fluid pressures. HUVECs were allowed to form a confluent monolayer before experimentation. There were four inbuilt experimental repeats (transwell assays) per experiment. The whole was repeated (×4) using HUVECS isolated from four different cords.

Experimental design

Medium in the upper chamber was replaced with 100 μl of dialysed (10 kDa dialysis tubing) fluorescein isothiocyanate-conjugated bovine serum albumin (FITC-BSA, 66 kDa; Thermo Fisher) in phenol-free M199 medium at a concentration of 1 mg/ml. After a 30-min equilibration, HUVECs were exposed to a single addition of recombinant human VEGF-A_{165}a (50 ng/ml), VEGF-A_{165}b (50 ng/ml) or PlGF (50 ng/ml). In further experiments, VEGF-A_{165}a (50 ng/ml) was followed by VEGF-A_{165}b (100 ng/ml), PlGF-2 (264-PG, R&D Systems 100 ng/ml) or both VEGF-A_{165}b (100 ng/ml) and PlGF-2 (100 ng/ml) in combination. Fifty microlitres of samples were collected from the lower compartment at 0, 30, 60, 90 and 120 min intervals, with the equivalent volume of fresh phenol-free M199 medium replenished after each sample collection. Samples were diluted in 50 μl of 0.1 M PBS and measured using a Thermo Fluoroskan Ascent F2 fluorescence plate reader at an emission/excitation wavelength of 495/520 nm. Concentrations of FITC–albumin in each sample were calculated via linear regression of a serial dilution series of the tracer. Total permeability of monolayers were calculated for each treatment based on the rate of solute flux (calculated in μg/min) over the first 30 min, the surface area of the monolayer, and the initial concentration difference between the upper and lower wells (1 mg/ml).

Immunostaining

After experimentation, monolayers were immediately fixed in 1% PFA. Cells were permeabilized with 0.15% Triton X-100 followed by blocking with 4% normal human serum in 0.1 M PBS for 30 min at RT. Monolayers were incubated with mouse anti-human CD144 (ThermoFisher) (VE-cadherin; 5 μg/ml) overnight at 4°C and FITC-conjugated goat anti-mouse IgG (Sigma-Aldrich, 20 μg/ml) for 2 h at 37°C in the dark after requisite washes.

Clinical Science (2017) **131** 2763–2775
https://doi.org/10.1042/CS20171252

Extra-corporeal perfusion of the placental microvascular bed

A well-established dual-perfusion procedure was employed [1,2,9-12]. To summarize, immediately after caesarean delivery, the placenta was transferred to a 37°C chamber with the umbilical cord kept clamped until cannulation to prevent loss of blood and collapse of feto-placental vessels. Within 20 min of arrival of the placenta, a vein and an artery supplying the microvascular bed of a randomly chosen intact cotyledon were each cannulated with a nasogastric (5 mm) tube to establish the fetal circulation. The placenta was inverted and the cotyledon was clamped in a Perspex chamber to isolate the lobule from the rest of the placenta. The independent maternal circulation was simulated by inserting five 5 mm nasogastric tubes into the intervillous space through the basal plate of the cotyledon, and drained through an exit tube in the Perspex chamber. Fetal and maternal circulations were connected to peristaltic pumps providing a constant 20 ml/min flow to the maternal circulation and a 5 ml/min flow to the fetal circulation, replicating the physiologic flow rates seen *in utero*. Establishment of both circulations were completed within 30 min of delivery to minimize hypoxic damage to the placenta. Perfusion was abandoned if fetal venous outflow was less than arterial inflow. From the 20 intact placenta recruited for the perfusion experiments, 15 allowed full perfusion (25% failure rate).

Experimental design

A 20-min open circuit equilibration period with oxygenated Medium 199 (Sigma, Poole, U.K.), with added sodium bicarbonate (2.2 g/l), albumin (5 g/l), high molecular weight dextran (2000 M_r; 8 g/l) and heparin (5000 IU/l) (final pH 7.2–7.4), was performed to reverse any post-parturition hypoxic changes [1]. After equilibration, fetal oxygenation was discontinued and both the maternal and foetal circulations were closed. Perfusion pressures were monitored and accepted if foetal pressure was between 40–80 mmHg and maternal pressure was between 18–20 mmHg [2].

Recombinant human VEGF-A_{165}a (20 ng/ml), VEGF-A_{165}b (20 ng/ml) or vehicle were introduced into the fetal circulation and the lobules perfused for 30 min. In reversal experiments, VEGF-A_{165}a exposure was followed by a separate VEGF-A_{165}b (40 ng/ml) perfusion (vehicle only acted as control) for an additional 30 min. Three different placentas were used for each experimental exposure. Tetramethylrhodamine isothiocyanate (TRITC)-conjugated dextran (76 M_r; Sigma, Dorset, U.K.), 1 mg/ml) was added as a bolus into the fetal circulation for the last 10 min of all perfusions (single growth factors or sequential VEGF isoform perfusions). The lobules were then perfusion fixed with 1% paraformaldehyde in 0.1 M phosphate buffer saline (pH 7.3) for 30 min. The lobule was excised and 10 mm^3 biopsies taken for a further immersion fixation (2 h). Biopsies were rinsed in PBS, cut into 5 mm^3 pieces, frozen in nitrogen-cooled isopentane (Fisher Scientific UK Limited, Loughborough, U.K.) and stored at −80°C until required.

Immunostaining

A minimum of six different blocks (randomly chosen) per placenta were cryo-sectioned and a minimum of six sections (5 μm thick) were taken from each block at different depths. Cryo-sections were air-dried and washed in 0.1 M PBS/BSA, before permeabilization with 0.15% Triton X-100 followed by blocking with 4% normal human serum in 0.1 M PBS for 30 min at room temperature. Sections were incubated overnight with mouse anti-human CD144 (VE-cadherin; 5 μg/ml) at 4°C and secondary antibodies as described before.

Microscopy and analysis

Transwell membranes and placental sections were visualized for expression of CD144 and TRITC-Dextran tracer using a Nikon LaboPhot-2 fluorescence microscope (Nikon, U.K.) and appropriate TRITC/FITC filters. Images (obtained by systematic random sampling of entire sections or membranes) from both channels were acquired using a Nikon Coolpix 995 camera (Nikon, U.K.).

Junctional integrity and tracer leakage analysis

Micrographs were analysed using Adobe Photoshop 6.0 (Adobe systems, U.K.). A pre-determined electronic grid was placed over each image and both VE-cadherin junction integrity and evidence of TRITC-Dextran tracer leakage quantified using systematic random sampling and unbiased 'forbidden line' counting principle to ensure that no vascular profile and paracellular cleft were counted twice [11]. For sampling efficiency, a minimum of 200 vascular profiles were counted from images per perfused placenta; c 600 vascular profiles were analysed for each experimental condition. For HUVEC monolayers, junctional integrity was determined by counting the % of paracellular clefts showing uniform VE-cadherin staining as a continuous thin line. Gaps in cell–cell adhesion regions with VE-cadherin negative cell edges were also counted. The % of cell–cell overlap showing thicker bands of VE-cadherin localization was noted. For placental sections, the total percentage of vascular profiles showing disrupted junctional VE-cadherin

(discontinuous staining or total loss) from paracellular clefts and associated tracer leakage (76 M_r Dextran-TRITC visualized as peri-vascular ablumenal fluorescent puncta or 'hotspots') was counted [11]. All experimental images from both HUVEC monolayers and placental sections were blinded to treatment regime before analyses.

Competitive binding ELISA

High-attachment 96-well ELISA plates (Corning, U.K.) were coated with recombinant Flt-1 overnight, and co-incubated with biotinylated-VEGF-A_{165}b (EC75), followed by non-biotinylated-VEGF-A_{165}a (0–160 nM) or PlGF (0–160 nM). Differences in VEGF binding to Flt-1 (n=12) were measured using streptavidin–HRP to biotin interactions, using a Thermo Fluoroskan Ascent F2 fluorescence plate reader at an absorbance wavelength of 450 nm.

Statistical analyses

All statistical analysis was carried out using GraphPad Prism. Comparisons of means were made using one-way ANOVA with Bonferroni's *post hoc* test.

Results

VEGF-A_{165}b inhibits VEGF-A_{165}a-mediated permeability in HUVECs

Incubation of HUVEC monolayers with VEGF-A_{165}a resulted in an increase in FITC–albumin tracer mass leakage over time (Figure 1A) compared with vehicle exposed cells. In contrast, incubation with VEGF-A_{165}b in isolation showed no change in FITC–albumin tracer mass permeate compared with vehicle over time. Co-incubation of VEGF-A_{165}b following 30 min of VEGF-A_{165}a exposure resulted in the inhibition of VEGF-A_{165}a-mediated increase in FITC–albumin tracer mass leak (Figure 1A).

Exposure to PlGF alone also resulted in no change in FITC–albumin tracer mass permeate with time (Figure 1B). Addition of PlGF after 30 min exposure to VEGF-A_{165}a did not prevent the VEGF-A_{165}a-mediated effects (see Figure 1B). Addition of PlGF alongside VEGF-A_{165}b prevented VEGF-A_{165}b-induced inhibition of VEGF-A_{165}a-mediated increase in FITC–albumin tracer mass leak (see Figure 1C). The calculated permeability values to FITC–albumin tracer reflected these observations, whereby exposure to VEGF-A_{165}a, but not VEGF-A_{165}b or PlGF significantly increased HUVEC monolayer permeability (P<0.001, Figure 1D). Similarly, VEGF-A_{165}a-mediated permeability increase was inhibited by VEGF-A_{165}b (P<0.001) but not PlGF (P>0.05). PlGF co-incubation with VEGF-A_{165}b abolished the rescue of the latter from VEGF-A_{165}a dependent increases in permeability (P<0.001) (Figure 1D).

VEGF-A_{165}a but not VEGF-A_{165}b or PlGF disrupts VE-cadherin junctions in HUVECs

VE-cadherin immunostaining demonstrated the presence of positive junctional cell–cell overlap regions and thin abutting junctions with continuous VE-cadherin staining (Figure 2) in control (vehicle only) experiments. Monolayers treated with VEGF-A_{165}a revealed observable endothelial junctional disruption after exposure (Figure 2B) with a decrease in continuous thin junctions and increase in discontinuities or total loss of VE-cadherin staining in cell–cell margins (described as gaps). This was not seen when monolayers were treated with VEGF-A_{165}b (Figure 2C) or PlGF (Figure 2D). Quantification (systematic random sampling) of the percentage of each type of VE-cadherin positive regions (Figure 2H) showed that there was a statistically significant decrease in the number of thin junctions showing continuous VE-cadherin occupancy (P<0.0001) after VEGF-A_{165}a exposure. VE-cadherin discontinuity within paracellular clefts increased with a significant increase in observable gaps (P<0.001). No significant change in both percentage of disrupted junctions and % of continuous VE-cadherin junctions were found in VEGF-A_{165}b or PlGF experiments when compared with controls (P>0.05, Figure 2H).

VEGF-A_{165}b prevented VEGF-A_{165}a-mediated VE-cadherin junctional disruption, which was inhibited by PlGF

VEGF-A_{165}b (Figure 2E), but not PlGF (Figure 2F), was able to prevent VEGF-A_{165}a-induced disruption of VE-cadherin junctions after 2-h exposure. However, addition of PlGF in combination with VEGF-A_{165}b (Figure 2G) prevented the observed VEGF-A_{165}b-mediated inhibition of VEGF-A_{165}a-induced junctional disruption. Analysis of percentage junctional integrity (Figure 2I) revealed a significant decrease in percentage of gaps after VEGF-A_{165}b co-incubation (P<0.0001) and an increase in percentage of thin continuous VE-cadherin junctions (P<0.01). No significant changes in either percentage gap or continuous VE-cadherin AJ staining were observed after PlGF

Clinical Science (2017) **131** 2763–2775
https://doi.org/10.1042/CS20171252

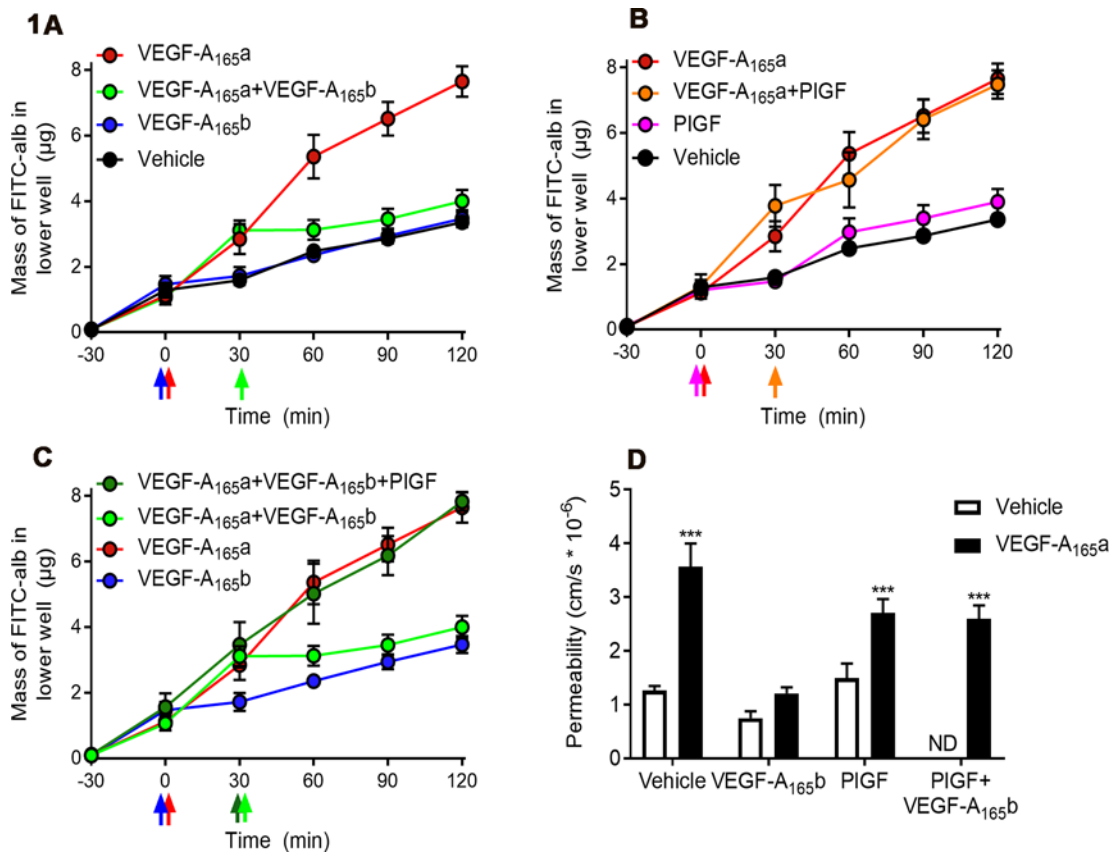

Figure 1. VEGF-A_{165}b inhibits VEGF-A_{165}a-mediated permeability increase in HUVEC monolayers

Graphs showing accumulation of FITC–albumin over time in transwell experiments (**A, B** and **C**) following exposure to VEGF-A_{165} isoforms, PlGF and vehicle only. Single VEGF additions were added at time = 0. Arrows indicate time of addition of VEGFs. (A) VEGF-A_{165}a (n=9, red trace) showing increase in tracer mass leakage over time compared with vehicle exposed cells (black). VEGF-A_{165}b (blue) shows similar leakage trace as vehicle. Addition of VEGF-A_{165}b (n=11) following 30 min of VEGF-A_{165}a exposure resulted in inhibition of this (green). (B) PlGF alone (n=7, magenta trace) did not increase tracer leakage, whilst co-incubation with VEGF-A_{165}a (orange) shows no inhibition of its activity (red). (C) Combination of all three growth factors (n=5, olive) shows increased FITC–albumin solute flux, similar to VEGF-A_{165}a alone. (**D**) Histograph showing the calculated permeability values of the HUVEC monolayers. VEGF-A_{165}a-mediated HUVEC permeability was inhibited by addition of VEGF-A_{165}b but not PlGF (X-axis). Co-incubation of PlGF with VEGF-A_{165}b abolished the VEGF-A_{165}b inhibition of VEGF-A_{165}a-dependent increase in permeability (***P<0.001 compared with vehicle); ND = not determined.

co-incubation (P>0.05). However, PlGF exposure in combination with VEGF-A_{165}b abolished the VEGF-A_{165}b inhibition of VEGF-A_{165}a-mediated effects (P>0.05) (see Figure 2I).

PlGF competes with VEGF-A_{165}b for binding to Flt-1

As the VEGF-A_{165}b inhibition of VEGF-A_{165}a mediated increased permeability was blocked by PlGF, which only binds VEGFR1 (flt-1), we hypothesized that this could occur if VEGF-A_{165}b was inhibiting VEGF-A_{165}a by signalling through VEGFR1. VEGF-A_{165}a and VEGF-A_{165}b compete for R1 [28], so we therefore determined the effect of PlGF on VEGF-A_{165}b binding to VEGFR1 using an Fc-VEGFR1 chimaeric protein. Incubation of Fc-VEGFR1 with un-labelled human recombinant VEGF-A_{165}b resulted in a concentration-dependent decrease in binding of biotinylated-VEGF-A_{165}b (EC75). Similarly, co-incubation with un-labelled PlGF resulted in an almost identical concentration-dependent decrease in biotinylated-VEGF-A_{165}b binding, with no significant difference in calculated IC_{50} between the two proteins (P>0.05) (see Figure 3), thus suggesting that the inhibition of VEGF-A_{165}a-mediated permeability by VEGF-A_{165}b could also be through its actions on VEGFR1.

Clinical Science (2017) **131** 2763–2775
https://doi.org/10.1042/CS20171252

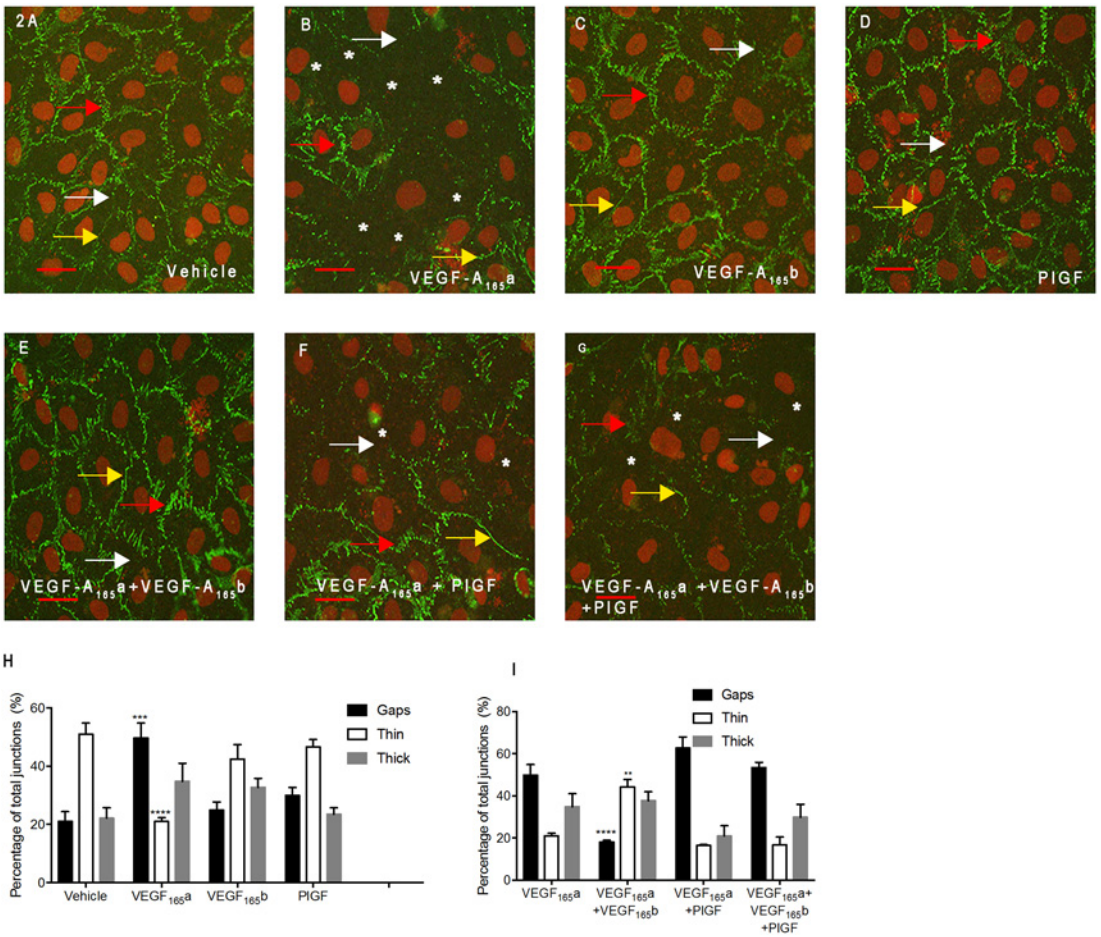

Figure 2. VEGF-A_{165}b inhibits VEGF-A_{165}a-induced disruption of VE-cadherin junctions

(**A**–**D**) Fluorescent micrographs showing VE-cadherin (green) immunolocalization in HUVEC monolayers treated with single additions of VEGF splice variants, PIGF or vehicle. (A) In control monolayers (vehicle treated), VE-cadherin was visualized as thick staining in cell–cell overlap regions (red arrow; thick junctions) and as continuous thin lines (yellow arrow) between cells. Some cell–cell boundaries revealed discontinuous staining (white arrow) or extensive loss of VE-cadherin staining (asterisk). Nuclei were stained with PI (red). (B) Monolayers treated with VEGF-A_{165}a showed increased numbers of cell–cell junctions with loss of or discontinuous VE-cadherin staining. This increase was not seen in monolayers exposed to VEGF-A_{165}b (C) or PlGF (D). (**E**–**G**) Fluorescent micrographs showing VE-cadherin immunostaining in HUVEC monolayers incubated with VEGF-A_{165}a and VEGF-A_{165}b (E) or PlGF (F) or both VEGF-A_{165}b + PlGF (G). VE-cadherin was found to show a continuous pattern of VE-cadherin staining similar to control (see A) when co-incubated with VEGF-A_{165}b (E). Disruption of VE-cadherin staining was observed in monolayers co-incubated with PlGF (F). Incubation with all three growth factors (G) resulted in persistence of discontinuous junctional profiles (asterisk, white arrows) seen for VEGF-A_{165}a alone; bar = 50 μm. (**H** and **I**) Quantitative analyses of VE-cadherin junctional occupancy after exposure to growth factors. (H) 2-h exposure to VEGF-A_{165}a (n=5) resulted in an increase in the percentage of junctions showing discontinuous or loss of junctional VE-cadherin (gaps, ***P<0.001) and decrease in the percentage of thin continuous VE-cadherin junctions (****P<0.0001) when compared with vehicle only study group. Both VEGF-A_{165}b (n=5) and PlGF (n=3) exposure did not change percentage junction integrity when compared with vehicle (P>0.05). The number of overlapping cell–cell regions (thick) was not found to be statistically different for the different treatments. (I) VEGF-A_{165}b co-incubation with VEGF-A_{165}a (n=5) decreased the percentage of junctions showing gaps (****P<0.0001) and increased the percentage of continuous VE-cadherin thin junctions (**P<0.01) compared with VEGF-A_{165}a. This was not seen in the PlGF co-incubation experimental group (n=3). However, PlGF in combination with VEGF-A_{165}b (n=3) abolished VEGF-A_{165}b inhibition of VEGF-A_{165}a-mediated effects.

Clinical Science (2017) **131** 2763–2775
https://doi.org/10.1042/CS20171252

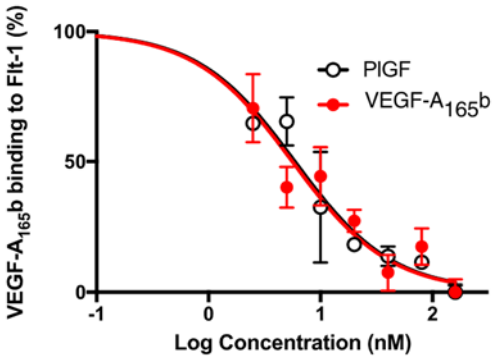

VEGF-A_{165}b (IC_{50})
5.6nM (3.8-8.3)
PlGF (IC_{50})
5.9nM (4.1-8.5)

Figure 3. PlGF competes with VEGF-A_{165}b for binding to Flt-1

Co-incubation of Fc-VEGFR1 with un-labelled VEGF-A_{165}b resulted in decreased binding of biotinylated-VEGF-A_{165}b (n=4). PlGF co-incubation equally inhibited biotinylated-VEGF-A_{165}b binding to Flt-1 binding (n=4) (ns = P>0.05).

VEGF-A_{165}a-mediated increased permeability and VE-cadherin disruption are prevented by VEGF-A_{165}b in the perfused human placental microvascular bed

Using the more physiological dual-perfusion system, addition of growth factors to the fetal microcirculation of term placental lobules resulted in observable differences in extravasation of TRITC-dextran (75 M_r) tracer (see Figure 4, right panel). VEGF-A_{165}a perfusions for 30 min resulted in a significant increase in percentage of vascular profiles associated with tracer leakage (71.2 ± 13.8%, Figures 4 and 5) compared with control perfusions (30.2 ± 4.4%; P<0.01). In contrast, perfusions of VEGF-A_{165}b saw no significant increase in percentage of leaky vessels (P>0.05) compared with control perfusions. Addition of VEGF-A_{165}b into the closed fetal circulation after a 30 min VEGF-A_{165}a perfusion period resulted in altered tracer leakage profile from that obtained with VEGF-A_{165}a only perfusions. Vascular profiles (9.4 ± 1.2%) were now found to be associated with peri-vascular 'hotspots' (P<0.05). This was not due to temporal recovery, as addition of vehicle only for 30 min after VEGF-A_{165}a perfusion showed no significant decrease in profiles expressing hotspots (P>0.05). Subsequent immunohistochemical analyses of the same sections revealed that tracer leakage matched disruption of VE-cadherin AJs (loss of VE-cadherin from paracellular clefts) (Figure 4, left panel). VEGF-A_{165}a-perfusion of placental microvascular beds resulted in a 49.3% decrease in vascular profiles showing VE-cadherin at paracellular clefts (P<0.01), while perfusions of VEGF-A_{165}b did not significantly alter VE-cadherin positive vascular profiles (86.7 ± 0.8%) compared with controls (89.3 ± 2.3%) (P>0.05). Sequential addition of VEGF-A_{165}b to VEGF-A_{165}a perfusions resulted in a recovery of junctional integrity with 81 ± 5% of vascular profiles showing VE-cadherin at paracellular clefts (P<0.05; Figure 5).

Discussion

These studies are the first to show that the anti-angiogenic VEGF-A_{165}b does not disturb the junctional occupancy of VE-cadherin or induce paracellular tracer leakage in the human placental microvascular bed and HUVEC monolayers. Indeed, VEGF-A_{165}b (at a 2-fold concentration) can block/reverse VEGF-A_{165}a-mediated increases in feto-placental endothelial permeability to macromolecules (75 kDa) and loss of VE-cadherin from AJs. In these experiments, PlGF did not affect endothelial integrity, VE-cadherin localization and permeability when added singly; however, it could prevent the rescue of VEGF-A_{165}a-mediated effects by VEGF-A_{165}b.

The similarities between the observed induced changes in both fetal endothelial cell cultures and the more physiological and complex perfused microvascular bed are re-assuring. Placental microvessels showed a robust response to a 30 min perfusion of exogenous VEGF-A_{165}a, with loss of VE-cadherin and increased vascular leak of 76 kDa

Clinical Science (2017) **131** 2763–2775
https://doi.org/10.1042/CS20171252

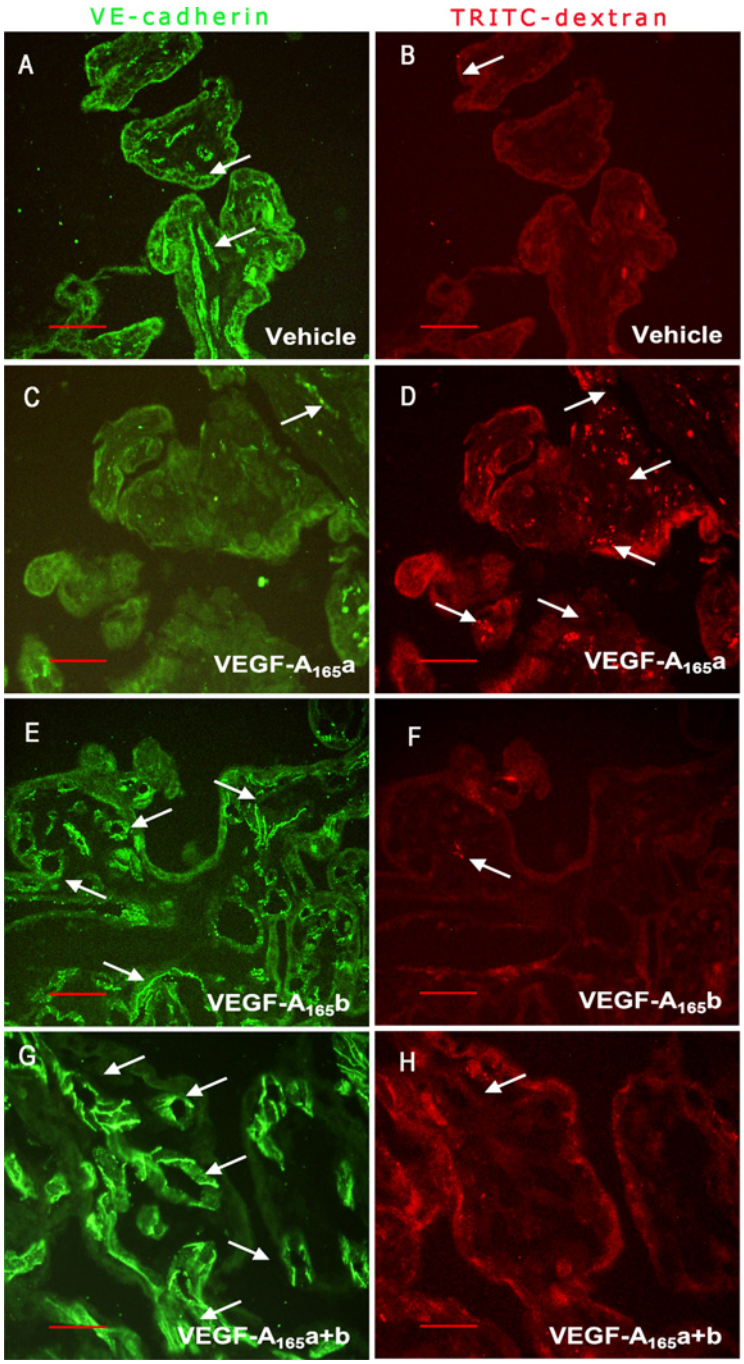

Figure 4. VEGF-A_{165}b reverses VEGF-A_{165}a-induced loss of junctional VE-cadherin and increased tracer leakage in perfused placental microvessels

Representative fluorescent micrographs of villous biopsies taken from perfused placental microvascular beds. Left panel shows VE–cadherin staining (FITC filter) whilst right panel shows the same image under TRITC filter to visualize any peri-vascular TRITC-dextran 'hotspots'; bar = 100 μm. (**A**) Image from control perfusion (vehicle only for 30 min) showing VE-cadherin positive microvascular profiles within placental villous trees. (**B**) No peri-vascular hotspots can be seen in the same villous trees. (**C**) Image showing a dramatic reduction in VE-cadherin positive vascular profiles following a 30 min perfusion with VEGF-A_{165}a. (**D**) Numerous tracer hotspots can now be seen trapped in the peri-vascular regions. (**E**) Image showing numerous VE-cadherin positive microvascular profiles in villous trees following perfusion with VEGF-A_{165}b for 30 min. (**F**) Note lack of or negligible presence of tracer hotspots in these villi. (**G**) Image from placenta perfused with VEGF-A_{165}a (30 min) followed by VEGF-A_{165}b (30 min) and tracer. VE-cadherin positive microvascular profiles are now a predominant feature, suggesting return of VE-cadherin to junctional regions. Concomitantly, there is minimal peri-vascular tracer 'hotspots' (**H**).

Clinical Science (2017) **131** 2763–2775
https://doi.org/10.1042/CS20171252

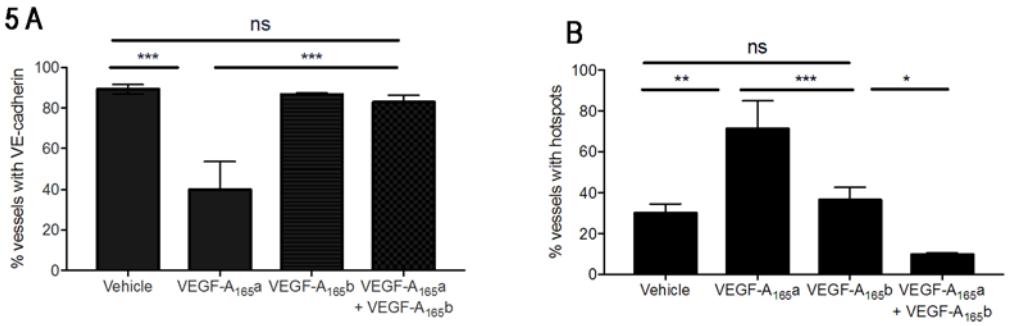

Figure 5. Quantitative analyses of VE-cadherin junctional occupancy and tracer leakage in perfused placental microvascular beds

(**A**) Systematic counts (from 600 vascular profiles per experimental condition) revealed that in perfused placental microvascular beds VEGF-A_{165}a significantly decreased the percentage of VE-cadherin positive vascular profiles compared with VEGF-A_{165}b or vehicle only (***$P<0.001$). VEGF-A_{165}b perfusion alone did not alter the % of VE-cadherin vascular profiles. In placentae where VEGF-A_{165}b was added after the 30 min VEGF-$_{165}$a perfusion, % of VE-cadherin vascular profiles was found to be similar to that of vehicle or VEGF-A_{165}b perfusions. (**B**) The % of vessels showing extravasation of TRITC-dextran was significantly increased in VEGF-A_{165}a study group (**$P<0.01$), but not altered when placentae were perfused with VEGF-A_{165}b when compared with vehicle only. VEGF-A_{165}b was able to reverse VEGF-A_{165}a-mediated permeability effects – the % of vascular profiles with associated peri-vascular hotspots was highly significantly reduced compared with VEGF-A_{165}a perfusions (***$P<0.001$). *=significant; **=very significant; ***=highly significant; ns=not significant.

dextrans. These changes were not induced when microvessels were perfused with VEGF-A_{165}b; indeed this splice variant could reverse the VEGF-A_{165}a-induced changes both in the perfusion model and in transwell experiments.

The monolayer permeability results are similar to those recently described in lung pulmonary endothelial cells [29], where VEGF-A_{165}a but not VEGF-A_{165}b was shown to increase monolayer permeability and decrease junctional integrity. However, they did not investigate the effect of PlGF on these cells.

The observed inability of either PlGF or VEGF-A_{165}b to alter VE-cadherin occupancy and AJ integrity in human placental microvessels and fetal endothelial cells may be due to their lack of neuropilin-1 binding property [22,26,30]. Neuropilin-1 is critical for VEGF-mediated endothelial permeability in human pulmonary endothelial cells and for pulmonary vascular leaks in inducible lung-specific VEGF transgenic mice [22]. Stable transfection of the neuropilin-1–VEGFR2 complex in endothelial cells resulted in decreased transendothelial resistance in a dose-dependent fashion following addition of VEGF-A_{165}a; this was not seen for single transfections of VEGFR2 or neuropilin-1 alone. Moreover, VEGF-A_{165}b prevents the formation of neuropilin–VEGFR2 complexes by VEGF-A_{165}a [31]. The reduction in VEGF-A_{165}a-mediated enhanced permeability in our studies may be due to competitive binding of VEGF-A_{165}b to the VEGFR2 receptor [25]. KDR occupancy by VEGF-A_{165}b may be followed by internalization but not the subsequent neuropilin-1 dependent re-shuttling of KDR to the membrane surface [32]. This therefore would rule out further VEGF-A_{165}a binding and triggering of phosphorylation events that lead to translocation of VE-cadherin from AJ domains. The recovery of junctional integrity seen in the sequential VEGF-A_{165}a + VEGF-A_{165}b perfusions, but not in VEGF-A_{165}a + vehicle perfusions argues that VEGF-A_{165}b is acting as an active signalling inhibitor. Our data allow one to hypothesize that the relative contributions of the two different VEGF-A_{165} isoforms may be an important driver behind the different feto-placental vascular permeability (and angiogenesis) observed for the different trimesters of pregnancy [9,10].

Plasma taken from pre-eclamptic mothers has been shown to induce transient increases in permeability in amphibian models, which was blocked by VEGF-A_{165}b specific neutralizing antibodies, and receptor tyrosine inhibitors at concentrations specific to VEGFR1 blockage [33]. This neutralizing antibody to VEGF-A_{165}b was shown to prevent the inhibition of VEGF-A_{165}b-mediated blockade of VEGF-A_{165}a-induced migration and cytoprotection of endothelial cells [34] and anti-angiogenesis in peripheral vascular disease [35]. This suggests that the pre-eclamptic plasma not only contained physiologically active VEGF-A_{165}b, but its action was incurred by altering the balance of VEGF-A_{165}b, PlGF and VEGF-A_{165}a, such that VEGF-A_{165}a was no longer able to induce the increase in permeability, potentially by binding heterodimers of VEGF-A_{165}b with either PlGF or VEGF-A_{165}a. Such heterodimers are theoretically possible but have not yet been clearly demonstrated.

PIGF did not increase AJ disruption or permeability of the fetal human umbilical vein endothelial cells. PIGF-1, but not PIGF-2, has been shown to stabilize VE-cadherin junctions after activation with VEGF in bovine retinal endothelial cells and after intra-vitreal injections in mouse, during a critical window [36]. The isoform used here was PlGF-2, which binds heparin and is therefore able to signal through VEGFR1 with heparin, indicating that full signalling does require the heparin binding domains. The PlGF-mediated abolition of VEGF-A_{165}b induced reversal of VEGF-A_{165}a-induced permeability was surprising. However, recent studies by Ganta et al. [37] have shown that VEGF-A_{165}b inhibits VEGF-A_{165}a-mediated signalling in adipose endothelial cells through inhibiting VEGFR1-mediated activation of the signal transducer and activator of transcription 3 (STAT3) pathway. It is therefore possible that VEGF-A_{165}b binds VEGFR1, inhibiting STAT3 signalling. When PlGF binds VEGFR1, even if it does not inhibit STAT3 signalling (or stimulate it), it prevents VEGF-A_{165}b from inhibiting it, so VEGF-A_{165}a would then be at liberty to increase permeability. There are currently no studies identifying whether PlGF signals through STAT3 or how it affects VEGF-A_{165}a-mediated STAT3 signalling, but it would appear that such studies are warranted.

In our HUVEC studies, when PlGF was added in combination with VEGF-A_{165}b, there was an abolition of the VEGF-A_{165}b-induced reversal of VEGF-A_{165}a-induced permeability. Whilst it is well known that VEGF-A_{165}a and PIGF can compete for VEGF-R1 binding [38], in the present study we have also shown that incubation of Fc-VEGFR1 with un-labelled PlGF resulted in a concentration-dependent decrease in biotinylated-VEGF-A_{165}b binding. Thus, addition of PIGF may have resulted in release of both splice variants. The excess VEGF-A_{165}a would then be at liberty to increase permeability via KDR–neuropilin signalling. Hetero-dimerization of PIGF with VEGF-A_{165}b could further assist VEGF-A_{165}a activity. Further studies are needed to understand the complex interplay between VEGF-A/PIGF and their receptors/co-receptors. Elucidation of the multiple signalling pathways, including whether/where the VEGFR1-linked angiogenic signalling pathway interacts with the VEGFR2-linked phosphorylation events that lead to disruption of VE-cadherin junctions is needed to understand how placental/fetal barrier function is regulated.

In summary, we have shown that VEGF-A_{165}b is able to inhibit vascular permeability induced by VEGF-A_{165}a *in vitro*, and in human placenta *ex vivo*, and that this is interfered with by placental growth factor. These results suggests that alterations in the ratio of these growth factors during normal placental development and in complicated pregnancies such as pre-eclampsia and diabetes would influence VE-cadherin clustering in fetal vessels and therefore placental barrier function, given that both the fetal endothelium and the syncytiotrophoblast act as resistance in series to materno-fetal hydrophilic solute transport.

Clinical perspectives

- The anti-angiogenic VEGF-A_{165}b isoform does not increase permeability in human placental microvessels or fetal endothelial cells.
- VEGF-A_{165}b isoform can interrupt VEGF-A_{165}a-induced permeability of feto-placental vessels.
- The interplay of the VEGF-A_{165} isoforms with PIGF suggests that the ratio of these three factors may be important in determining the placental endothelial barrier and therefore fetal well-being in normal and complicated pregnancies.

Funding

This work was supported by the British Heart Foundation [grant number PG/13/85/30536]. We would like to thank clinical staff and midwives at the Labour Ward, Queens Medical Centre, Nottingham University Hospital for the timely retrieval of placenta.

Competing Interests

The authors declare that there are no competing interests associated with the manuscript.

Author Contribution

V.P. performed most of the experiments, statistical analyses and was involved in writing the manuscript. L.L. and D.O.B. co-designed and co-directed the study and were involved in manuscript writing. L.L. assisted with the placental perfusions, directed analyses of the tracer leakage and VE-cadherin dynamics. All authors reviewed the manuscript.

Clinical Science (2017) **131** 2763–2775
https://doi.org/10.1042/CS20171252

Abbreviations

AJ, adherens junction; FITC-BSA, fluorescein isothiocyanate-conjugated bovine serum albumin; Flt-1, Fms-like tyrosine kinase; HUVEC, human umbilical vascular endothelial cell; KDR, kinase insert domain receptor; PI, propidium iodide; PIGF, placental growth factor; PFA, para-formaldehyde; sFlt-1, soluble fms-like tyrosine kinase; STAT3, signal transducer and activator of transcription 3; TRITC, tetramethylrhodamine isothiocyanate; VE-cadherin, vascular endothelial-cadherin; VEGF, vascular endothelial growth factor; VEGFR1, vascular endothelial growth factor receptor-1; VEGFR2, vascular endothelial growth factor receptor-2.

References

1 Leach, L. and Firth, J.A. (1992) Fine structure of the paracellular junctions of terminal villous capillaries in the perfused human placenta. *Cell Tissue Res.* **268**, 447–452
2 Eaton, B.M., Leach, L. and Firth, J.A. (1993) Permeability of the fetal villous microvasculature in the isolated perfused term human placenta. *J. Physiol. (Lond.)* **463**, 141–155
3 Leach, L., Clark, P., Lampugnani, M.G., Arroyo, A.G., Dejana, E. and Firth, J.A. (1993) Immunoelectron characterisation of the inter-endothelial junctions of human term placenta. *J. Cell Sci.* **104**, 1073–1081
4 Dejana, E., Orsenigo, F. and Lampugnani, M.G. (2008) The role of adherens junctions and VE-cadherin in the control of vascular permeability. *J. Cell Sci.* **121**, 2115–2122
5 Gavard, J. (2013) Endothelial permeability and VE-cadherin: a wacky comradeship. *Cell Adhes. Migr.* **7**, 455–461
6 Esser, S., Lampugnani, M.G., Corada, M., Dejana, E. and Risau, W. (1998) Vascular endothelial growth factor induces VE-cadherin tyrosine phosphorylation in endothelial cells. *J. Cell Sci.* **111**, 1853–1865
7 Wessel, F., Winderlich, M., Holm, M., Frye, M., Rivera-Galdos, R., Vockel, M. et al. (2014) Leukocyte extravasation and vascular permeability are each controlled in vivo by different tyrosine residues of VE-cadherin. *Nat. Immunol.* **15**, 223–230
8 Demir, R., Seval, Y. and Huppertz, B. (2007) Vasculogenesis and angiogenesis in the early human placenta. *Acta Histochem.* **109**, 257–265
9 Leach, L., Babawale, M.O., Anderson, M. and Lammiman, M. (2002) Vasculogenesis, angiogenesis and the molecular organisation of endothelial junctions in the early human placenta. *J. Vasc. Res.* **39**, 246–259
10 Leach, L., Lammiman, M.J., Babawale, M.O., Hobson, S.A., Bromilou, B., Lovat, S. et al. (2000) Molecular organization of tight and adherens junctions in the human placental vascular tree. *Placenta* **21**, 547–557
11 Leach, L., Gray, C., Staton, S., Babawale, M.O., Gruchy, A., Foster, C. et al. (2004) Vascular endothelial cadherin and beta-catenin in human fetoplacental vessels of pregnancies complicated by Type 1 diabetes: associations with angiogenesis and perturbed barrier function. *Diabetologia* **47**, 695–709
12 Babawale, M.O., Lovat, S., Mayhew, T.M., Lammiman, M.J., James, D.K. and Leach, L. (2000) Effects of gestational diabetes on junctional adhesion molecules in human term placental vasculature. *Diabetologia* **43**, 1185–1196
13 Wang, Y., Lewis, D.F., Gu, Y., Zhang, Y., Alexander, J.S. and Granger, D.N. (2004) Placental trophoblast-derived factors diminish endothelial barrier function. *J. Clin. Endocrinol. Metab.* **89**, 2421–2428
14 Bates, D.O., MacMillan, P.P., Manjaly, J.G., Qiu, Y., Hudson, S.J., Bevan, H.S. et al. (2006) The endogenous anti-angiogenic family of splice variants of VEGF, VEGFxxxb, are down-regulated in pre-eclamptic placentae at term. *Clin. Sci. (Lond.)* **110**, 575–585
15 Carmeliet, P., Moons, L., Luttun, A., Vincenti, V., Compernolle, V., De Mol, M. et al. (2001) Synergism between vascular endothelial growth factor and placental growth factor contributes to angiogenesis and plasma extravasation in pathological conditions. *Nat. Med.* **7**, 575–583
16 Levine, R.J., Maynard, S.E., Qian, C., Lim, K.H., England, L.J., Yu, K.F. et al. (2004) Circulating angiogenic factors and the risk of preeclampsia. *N. Engl. J. Med.* **350**, 672–683
17 Benton, S.J., Hu, Y., Xie, F., Kupfer, K., Lee, S.W., Magee, L.A. et al. (2012) Can placental growth factor in maternal circulation identify fetuses with placental intrauterine growth restriction? *Am. J. Obstet. Gynecol.* **206**, 163:e1–7, doi.org/10.1016/j.ajog.2011.09.019
18 Benton, S.J., McCowan, L.M., Heazell, A.E., Grynspan, D., Hutcheon, J.A., Senger, C. et al. (2016) Placental growth factor as a marker of fetal growth restriction caused by placental dysfunction. *Placenta* **42**, 1–8
19 Mizuuchi, M., Cindrova-Davies, T., Olovsson, M., Charnock-Jones, D.S., Burton, G.J. and Yung, H.W. (2016) Placental endoplasmic reticulum stress negatively regulates transcription of placental growth factor via ATF4 and ATF6beta: implications for the pathophysiology of human pregnancy complications. *J. Pathol.* **238**, 550–561
20 Eriksson, A., Cao, R., Pawliuk, R., Berg, S.M., Tsang, M., Zhou, D. et al. (2002) Placenta growth factor-1 antagonizes VEGF-induced angiogenesis and tumor growth by the formation of functionally inactive PlGF-1/VEGF heterodimers. *Cancer Cell* **1**, 99–108
21 Bates, D.O. and Harper, S.J. (2002) Regulation of vascular permeability by vascular endothelial growth factors. *Vascul. Pharmacol.* **39**, 225–237
22 Becker, P.M., Waltenberger, J., Yachechko, R., Mirzapoiazova, T., Sham, J.S., Lee, C.G. et al. (2005) Neuropilin-1 regulates vascular endothelial growth factor-mediated endothelial permeability. *Circ. Res.* **96**, 1257–1265
23 Kawamura, H., Li, X., Harper, S.J., Bates, D.O. and Claesson-Welsh, L. (2008) Vascular endothelial growth factor (VEGF)-A165b is a weak in vitro agonist for VEGF receptor-2 due to lack of coreceptor binding and deficient regulation of kinase activity. *Cancer Res.* **68**, 4683–4692
24 Bates, D.O., Cui, T.G., Doughty, J.M., Winkler, M., Sugiono, M., Shields, J.D. et al. (2002) VEGF165b, an inhibitory splice variant of vascular endothelial growth factor, is down-regulated in renal cell carcinoma. *Cancer Res.* **62**, 4123–4131
25 Woolard, J., Wang, W.Y., Bevan, H.S., Qiu, Y., Morbidelli, L., Pritchard-Jones, R.O. et al. (2004) VEGF165b, an inhibitory vascular endothelial growth factor splice variant: mechanism of action, in vivo effect on angiogenesis and endogenous protein expression. *Cancer Res.* **64**, 7822–7835

26 Cebe Suarez, S., Pieren, M., Cariolato, L., Arn, S., Hoffmann, U., Bogucki, A. et al. (2006) A VEGF-A splice variant defective for heparan sulfate and neuropilin-1 binding shows attenuated signaling through VEGFR-2. *Cell. Mol. Life Sci.* **63**, 2067–2077
27 Autiero, M., Luttun, A., Tjwa, M. and Carmeliet, P. (2003) Placental growth factor and its receptor, vascular endothelial growth factor receptor-1: novel targets for stimulation of ischemic tissue revascularization and inhibition of angiogenic and inflammatory disorders. *J. Thromb. Haemostasis* **1**, 1356–1370
28 Hua, J., Spee, C., Kase, S., Rennel, E.S., Magnussen, A.L., Qiu, Y. et al. (2010) Recombinant human VEGF165b inhibits experimental choroidal neovascularization. *Invest. Ophthalmol. Vis. Sci.* **51**, 4282–4288
29 Ourradi, K., Blythe, T., Jarrett, C., Barratt, S.L., Welsh, G.I. and Millar, A.B. (2017) VEGF isoforms have differential effects on permeability of human pulmonary microvascular endothelial cells. *Respir. Res.* **18**, 116
30 Migdal, M., Huppertz, B., Tessler, S., Comforti, A., Shibuya, M., Reich, R. et al. (1998) Neuropilin-1 is a placenta growth factor-2 receptor. *J. Biol. Chem.* **273**, 22272–22278
31 Delcombel, R., Janssen, L., Vassy, R., Gammons, M., Haddad, O., Richard, B. et al. (2013) New prospects in the roles of the C-terminal domains of VEGF-A and their cooperation for ligand binding, cellular signaling and vessels formation. *Angiogenesis* **16**, 353–371
32 Ballmer-Hofer, K., Andersson, A.E., Ratcliffe, L.E. and Berger, P. (2011) Neuropilin-1 promotes VEGFR-2 trafficking through Rab11 vesicles thereby specifying signal output. *Blood* **118**, 816–826
33 Bills, V.L., Salmon, A.H., Harper, S.J., Overton, T.G., Neal, C.R., Jeffery, B. et al. (2011) Impaired vascular permeability regulation caused by the VEGF(1)(6)(5)b splice variant in pre-eclampsia. *BJOG* **118**, 1253–1261
34 Magnussen, A.L., Rennel, E.S., Hua, J., Bevan, H.S., Beazley Long, N., Lehrling, C. et al. (2010) VEGF-A165b is cytoprotective and antiangiogenic in the retina. *Invest. Ophthalmol. Vis. Sci.* **51**, 4273–4281
35 Kikuchi, R., Nakamura, K., MacLauchlan, S., Ngo, D.T., Shimizu, I., Fuster, J.J. et al. (2014) An antiangiogenic isoform of VEGF-A contributes to impaired vascularization in peripheral artery disease. *Nat. Med.* **20**, 1464–1471
36 Cai, J., Wu, L., Qi, X., Shaw, L., Li Calzi, S., Caballero, S. et al. (2011) Placenta growth factor-1 exerts time-dependent stabilization of adherens junctions following VEGF-induced vascular permeability. *PLoS One* **6**, e18076
37 Ganta, V.C., Choi, M., Kutateladze, A. and Annex, B.H. (2017) VEGF165b modulates endothelial VEGFR1-STAT3 signaling pathway and angiogenesis in human and experimental peripheral arterial disease. *Circ. Res.*, **in press**
38 Park, J.E., Chen, H.H., Winer, J., Houck, K.A. and Ferrara, N. (1994) Placenta growth factor. Potentiation of vascular endothelial growth factor bioactivity, in vitro and in vivo, and high affinity binding to Flt-1 but not to Flk-1/KDR. *J. Biol. Chem.* **269**, 25646–25654